

Research Article

Evaluation of Novel Anti-VEGF Molecules in the Animal Model of Human Lung Cancer

Sanjukta Chakrabarti¹, Colin J. Barrow², Rupinder K. Kanwar³, Venkata Ramana^{1*}, Rakesh N. Veedu^{4,5} and Jagat R. Kanwar^{3*}

¹Reliance Life Sciences, Dhirubhai Ambani Life Sciences Center, Navi Mumbai 400701, India; ²School of Life and Environmental Sciences, Deakin University, Waurn Ponds Campus, Geelong 3216, Australia; ³Nanomedicine-Laboratory of Immunology and Molecular Biomedical Research (NLIMBR), School of Medicine (SoM), Centre for Molecular and Medical Research (C-MMR), Deakin University, Waurn Ponds Campus, Geelong 3216, Australia; ⁴Centre for Comparative Genomics, Murdoch University, Perth, 6150 Australia; ⁵Perron Institute for Neurological and Translational Science, Nedlands, Perth, 6009, Australia.

Abstract | Abnormal angiogenesis or the formation of aberrant vasculature in humans, may lead to various pathological conditions including tumor development. The most important factor implicated in the angiogenic processes is vascular endothelial growth factor (VEGF) protein and its family of ligands and receptors (VEGFRs). Survival, proliferation, migration and invasion of endothelial cells which give rise to the vascular network, is mediated through VEGF/VEGFR activation of the signal transduction pathways. Thus blocking VEGF is an efficient strategy for blocking tumor angiogenesis. Several anti-VEGF drugs have been developed over the last two decades and some are still at different development stages of pre-clinical and clinical trials. In this study, we explored the anti-angiogenic properties of three anti-VEGF molecules such as two fusion proteins, VEGF Trap_{R1R2} and VEGFR1(D1-D3)-Fc, and one DNA aptamer, RNV66, in an *in vivo* model of human A549 lung cancer. VEGF Trap_{R1R2} is a commercial anti-angiogenic fusion protein. Our earlier studies demonstrated the anti-angiogenic and anti-proliferative activities of VEGFR1(D1-D3)-Fc and RNV66 in *in vitro* functional assays. We compared the anti-tumorigenic properties of these three molecules for tumor volume reduction in xenotransplanted SCID mice and by histopathological and immunohistochemical analyses. Our results demonstrated that fusion protein VEGFR1(D1-D3)-Fc efficiently inhibited the lung cancer growth *in vivo*. Although the aptamer RNV66 was not found to be as efficient in this study, the results were also not surprising as the aptamer was administered naked and at low dose. As these are only our preliminary studies, a detailed investigation is planned using multiple doses, chitosan nanoparticle conjugated aptamer inline with the previous report on RNV66, and an approved VEGF inhibitor Avastin. Overall, the findings highlight that VEGFR1(D1-D3)-Fc can also serve as a potential anti-angiogenic molecule.

Editor | Dr. Tarun Kumar Sharma, Centre for Biodesign and Diagnostics, NCR Biotech Science Cluster, 3rd Milestone, Faridabad-Gurgaon Expressway, Faridabad, India.

Received | April 20, 2016; **Accepted** | June 24, 2017; **Published** | November 04, 2017

***Correspondence** | Venkata Ramana, Dhirubhai Ambani Life Sciences Center, Navi Mumbai 400701, India; **Email:** venkata.ramana@relbio.com; Jagat R. Kanwar, Centre for Molecular and Medical Research (C-MMR), Deakin University, Waurn Ponds Campus, Geelong 3216, Australia; **Email:** jagat.kanwar@deakin.edu.au

Citation | Chakrabarti, S., Barrow, C.J., Kanwar, R.K., Ramana, V., Veedu, R.N. and Kanwar, J.R. 2017. Evaluation of novel anti-VEGF molecules in the animal model of human lung cancer. *Aptamers and Synthetic Antibodies*, 3(1): 74-93.

Keywords | Anti-VEGF Molecules, Human lung cancer, Cancer, Abnormal angiogenesis

Introduction

Vascular endothelial growth factor (VEGF) is a critical and specific mitogen and signaling pro-

tein that stimulates the growth of vascular endothelial cells (Hoeben, et al., 2004). VEGF is produced by endothelial cells as well as non-endothelial cells such as macrophages, activated T cells, platelets, keratino-

cytes and a variety of tumor-associated stromal cells (Duffy et al., 2004). It is a cytokine which transmits activating, proliferative and chemotactic signals from hypovascularized tissues to endothelial cells of quiescent blood vessels and initiates new vessel sprouting to increase perfusion of the target tissue. There are seven related glycoprotein members of the VEGF family, which include VEGF-A, VEGF-B, VEGF-C, VEGF-D, VEGF-E, VEGF-F and PlGF (Takahashi and Shibuya, 2005). Human VEGF-A has nine isoforms, resulting from alternative splicing of VEGF-A mRNA, including VEGF₁₂₁, VEGF₁₄₅, VEGF₁₄₈, VEGF₁₆₂, VEGF₁₆₅, VEGF_{165b}, VEGF₁₈₃, VEGF₁₈₉ and VEGF₂₀₆, of which VEGF₁₆₅ is the most abundant and potent isoform (De Almodovar et al., 2009). This heparin binding-growth factor promotes creation of new blood vessels after injury, muscle following exercise, and new vessels collateral circulation to bypass blocked vessels (Bainbridge et al., 2002).

VEGF is the primary and most well-studied inducer of angiogenesis. Angiogenesis, or the process of formation and maintenance of new blood vessels from previously existing ones is tightly regulated by pro and anti-angiogenic factors. Abnormal angiogenesis, where pro-angiogenic factors are actively involved, results in aberrant vasculature leading to various pathological conditions. In addition to playing a part in normal physiological process of blood vessel formation, VEGF also plays a crucial role in pathological angiogenesis, including tumor angiogenesis and other diseases related to neovascularization such as rheumatoid arthritis (Elshabrawy et al., 2015) psoriasis (Guerard and Pouliot et al., 2012) and age-related macular degeneration (Tombran-Tink and Barnstable, 2007; Rajappa et al., 2010; Rubio and Adamis, 2015). In cancer, the growing tumor secretes a plethora of soluble factors including VEGF, which when coupled to hypoxia, are responsible for upregulation of a number of genes, which together play an important role in tumor angiogenesis and cancer metastasis (Krock et al., 2011). VEGF induces expression of several enzymes including matrix metalloproteinases (MMPs), which help in matrix degradation, cellular migration and invasion (Ghosh et al., 2012; Rundhaug, 2003). That VEGF acts as an intracrine cell survival factor in cancerous cells, has been shown in its role in colorectal cancer, where depleting VEGF resulted in decreased cell survival and increased sensitivity to chemotherapy (Bhattacharya et al., 2016).

VEGF stimulates endothelial cells by binding to

its cell surface tyrosine kinase receptors (VEGFR1, VEGFR2 and VEGFR3) with different binding affinities, tissue distributions, cellular functions and signal transduction properties. VEGFR1 is the receptor for VEGF-A, VEGF-B and PlGF, whereas VEGFR2 binds VEGF-A, VEGF-C and VEGF-D. VEGFR3, found primarily on lymphatic endothelial cells, binds to VEGF-C and VEGF-D with high affinity and is responsible for the growth, development and maintenance of lymph vessels. VEGFR1 is expressed on vascular endothelial cells and other cell types such as neutrophils, monocytes, macrophages, hepatocytes, hematopoietic stem cells, vascular smooth muscle cells, pericytes and endothelial progenitor cells. It is implicated in modulation of vascular development during later stages of embryogenesis, since its gene deletion resulted in mice that are unable to properly assemble blood vessels. The functions of VEGFR1 include induction of MMPs, regulation of hematopoiesis, and recruitment of monocytes. VEGFR2 is expressed predominantly on angiogenic vascular endothelial cells and bone marrow derived cells that directly or indirectly contribute to the formation of blood vessel walls. Deletion of VEGFR2 gene suppresses endothelial precursor cell function and inhibits primary vascular plexus formation in vasculogenesis, leading to embryonic lethality at early stages (De Oliveira et al., 2011). Although VEGFR1 binds to VEGF with 10fold higher affinity than that of VEGFR2 (Kd = 10-30 pM vs. 75-300 pM), it exhibits 10-fold lower kinase activity (Smith et al., 2015) and hence, most of the vascular effects of the ligand seem to be mediated by the activation of VEGFR2, which acts *via* Raf-Mek-Erk mediated signal transduction pathway for cell proliferation. For endothelial cell survival, VEGF-VEGFR2 interaction induces PI3 kinase-Akt signaling pathway and also expression of anti-apoptotic proteins including Bcl-2 (Pidgeon et al., 2001), XIAP (Kim et al., 2008) and surviving (Kanwar et al., 2013).

The VEGF/VEGFR pathway is the best characterized pathway governing angiogenesis and blocking this pathway offers potential therapeutic targets against diseases where angiogenesis plays a critical pathological role (Indraccolo and Mueller-Klieser, 2016). Targeting VEGF or its downstream effectors by inhibiting VEGF binding to its key physiological receptor should impede angiogenesis, which can be therapeutic benefit.

Several anti-angiogenic drugs are being tested globally in several clinical trials sponsored by various phar-

maceutical and biotech companies, medical centers and national institutes. Anti-angiogenic class of drugs can act not only in a broad range of cancers, but in a much broader way to treat several diseases other than cancer where abnormal vasculature development plays a critical role in either causation or progression. Most of these drugs display their tumor-inhibitory activity through the VEGF/VEGFR system. They are relatively less toxic compared to anti-cancer drugs as they target only normal endothelial cells, thereby minimizing the harmful side effects of chemotherapy, which kills normal cells along with tumor cells. The strategy of blocking cellular VEGF is by far the most effective anti-angiogenic strategy in terms of efficacy. Several anti-VEGF molecules have been developed or in different phases of development, including monoclonal antibodies, aptamers, siRNA, antisense oligonucleotides, catalytic oligonucleotides including ribozymes and DNAzymes, transcription decoys, receptor decoys, fusion proteins and peptidomimetics (Chakrabarti et al., 2014).

The current study explores the anti-VEGF and thus anti-angiogenic activities of two experimental anti-VEGF molecules, and a molecule with established activity, in mouse model of human lung carcinoma. The first molecule is an anti-VEGF recombinant Fc-fusion protein while the other is a DNA aptamer. Fc-fusion protein, VEGF Trap_{R1R2} was used as a positive control to compare the biological activities of the experimental molecules. Earlier studies have proven the efficacy of these molecules *in vitro* (Chakrabarti et al., 2016; Roy et al., 2015). Inhibition of VEGF₁₆₅-induced endothelial cell proliferation and capillary network formation in HUVEC by VEGFR1(D1-D3)-Fc was demonstrated in bioassays.

Aptamers belong to a special class of small nucleic acid molecules (DNA or RNA) capable of forming secondary and tertiary structures and possessing very high binding affinity to specific cellular protein targets. Aptamers are chemically synthesized, and are considered to be the chemical equivalent of antibodies owing to their high target specificity and affinity. They are also non-immunogenic due to their relatively small size and considered as potential targeting ligands as they are easy to synthesize and modify for conjugating to other drugs or carriers (Ni et al., 2011). Aptamers are synthesized *in vitro* by a technology called Systematic Evolution of Ligands by EXponential enrichment (SELEX). Owing to their high speed of generation, scale up and batch-to-batch

reproducibility, ultra-high affinity, specificity, stability and regenerability, as well as simplicity in functional modification with various types of molecules like nanomaterials and fluorophores, aptamers have found wide range of applications in diagnostics, biosensors and therapeutics. They are also in the competition with antibodies in electrochemical sensors and colorimetric detection systems (Abhijeet et al., 2017). Owing to their small size and flexibility, aptamers have tremendous potential in binding to targets unreachable by antibodies and small molecules, in the field of cancer immunology, antitoxins and targeted drug delivery. They can also be used in the treatment of viral infection owing to their ease and pace of synthesis and lower cost, keeping up with the rapidly mutated viral strains (Zhou and John, 2016). Moreover, aptamer generation eliminates the use of host animals which further brings down the cost (Sharma et al., 2017).

The global market for aptamers is rapidly growing at an annual growth rate of 17.89 % and is predicted to reach US \$244.93 million by 2020 from US \$107.56 million in 2015. Aptamers have a huge potential. Pegaptinib (Macugen[®]) was the first aptamer drug to be therapeutically approved by USFDA in 2004. It is an RNA aptamer targeting VEGF-A isoforms (VEGF₁₆₅ and VEGF₁₂₁) and used for treating choroidal neovascularization in age related macular degeneration (AMD) (Ng et al., 2006). Another anti-VEGF DNA aptamer, V7t1, was modified by using a locked nucleic acid (LNA) incorporation into the unmodified DNA aptamer. When LNA, a chemically modified nucleic acid analogue was incorporated into V7t1, a stable G-quadruplex structure with a single conformation was induced, and the resulting LNA-modified DNA aptamer, RNV66, had a much higher target binding affinity and increased nuclease resistance (Edwards et al., 2015). Figure 1 shows the structure of aptamer RNV66 that was successful in blocking cell proliferation of human umbilical vein endothelial cells (HUVEC) as well as inhibit colony formation in MCF-7, breast cancer cells, *in vivo*. RNV66 also effectively inhibited proliferation of triple negative breast cancer cell lines, MDA-MB-231 and HS578T in cell viability assays. Inhibition of proliferation of HeLa, cervical cancer cell line by RNV66, further revealed the efficacy of the aptamer towards other solid tumors. *In vivo* studies with mouse breast tumor (4T1) model demonstrated that RNV66 effectively caused inhibited the breast cancer progression in mice, while a combination of RNV66 with doxorubicin and taxol completely eliminated the tumor.

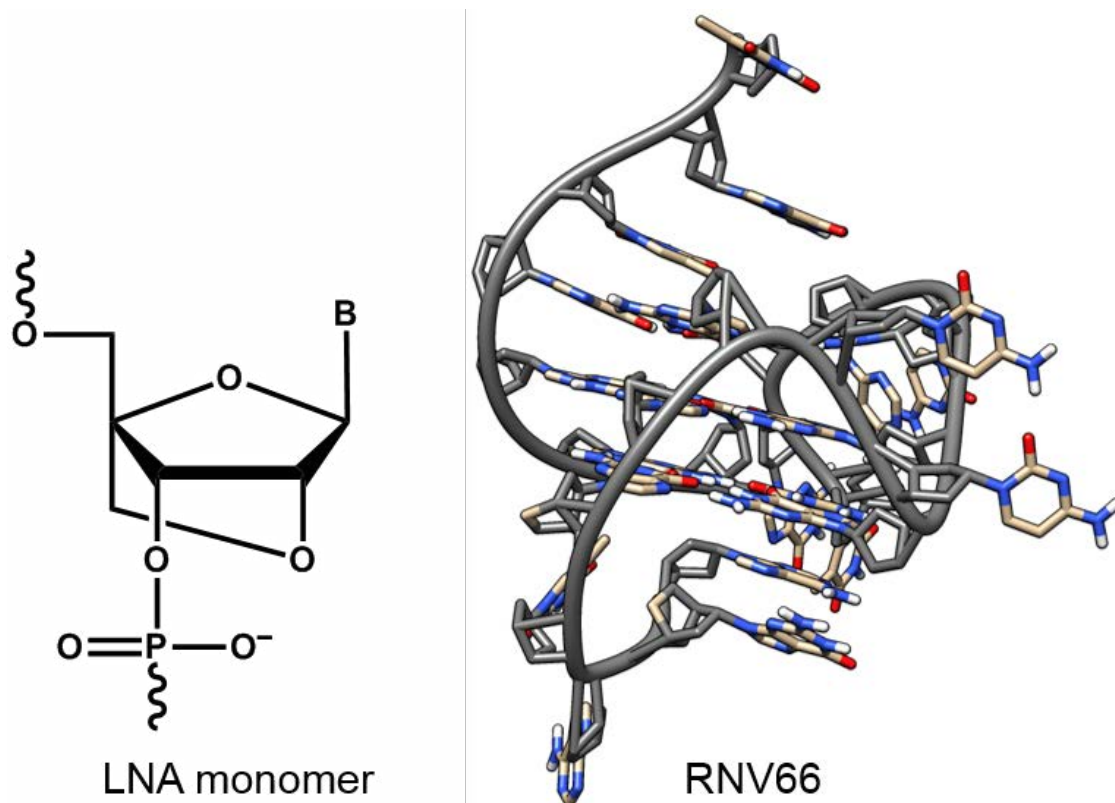


Figure 1: Structure of the aptamer, RNV66 (Edwards, S.L. et al. *Chemical Communications*; 2015) LNA stands for locked nucleic acid. It is a novel class of high-affinity RNA analogue in which the ribose ring is locked by a methylene bridge to 3'-endo conformation, giving it very high thermal stability. The aptamer RNV66 contains 3 LNA bases.

The other anti-VEGF molecule whose anti-angiogenic efficacy was assessed in the current study, *in vivo*, was VEGFR1 (D1-D3)-Fc, a recombinant Fc-fusion protein. This molecule was developed containing the first three immunoglobulin-like extracellular domains of VEGFR1 (D1, D2 and D3), which are the minimal and necessary domains for ligand (VEGF) binding, fused to Fc portion (hinge-CH2-CH3) region of human IgG1. Five amino acids (EPKSC) from the twelve residues present in IgG1 hinge region were removed as observed in commercial VEGF Trap_{R1R2} (aflibercept) construct.

In vivo efficacy of the two molecules were compared to the efficacy of aflibercept by first developing A549 human lung tumors in SCID mice, followed by treating the xenograft-bearing mice with specific doses of the drugs and subsequently by evaluating the effects of treatment in mice. After the end of treatment, the mice were sacrifice and tumors excised. Tumor dimensions were measured to assess any reduction in tumor volume. Tumor sections were subjected to histopathology (HandE) and immunohistochemistry (IHC) analyses. Figure 2 gives the schematic representation of different antigen detection methods used in IHC. Gross examination of HandE stained tumor

section were performed to indicate necrotic and neoplastic areas, as well as extent of neo-angiogenesis inhibition. In IHC, cell proliferation marker, Ki-67, was used to determine overall status of proliferating cells in excised tumors. Immunohistochemistry with fluorescence detection was used to detect presence of angiogenesis marker, CD31, on vascular endothelial lining of mice blood vessels supporting human tumor xenograft (Ghanekar et al., 2013; Montecinos et al., 2012).

Materials and Methods

Animals and cell line

Sixteen male and nineteen female SCID mice used for the study, were sourced from Animal Breeding and Housing Facility, Laboratory Animal research Services (LARS), Reliance Life Sciences, Navi Mumbai, India. The mice were maintained in pathogen-free conditions and well fed. All experimentation involving laboratory animals were approved by the Institutional Animal Ethics Committee (IAEC) [Registration number 423/01/a/CPCSEA; Protocol number: 20/15; Date of approval: 08 June 2015]. Human lung adenocarcinoma alveolar basal epithelial cells, A549 (Catalogue# CCL-185; ATCC, Manassas, Virginia,

USA) were used to generate tumors in this murine model of human cancer. Cancer cells were cultured in Dulbecco's Modified Eagle Medium (DMEM) medium supplemented with 10% fetal calf serum and 1% penicillin-streptomycin in 5% CO₂ at 37°C. Five million cells were mixed with 50 µL DMEM medium and suspended in 50 µL Matrigel (catalogue# 356231; Corning, New York, USA) were injected sub-cutaneously in the right flank of each of the experimental animal. SCID mice used for the study were 4-7 weeks old. All animals developed single palpable tumors within second to third week of injection of cells and size of the developing tumors in mice xenotransplanted with A549 tumor cells were measured externally using digital calipers every three days. Tumor volumes were calculated using the modified ellipsoidal formula: $\text{Volume} = (\text{Length} \times \text{Width}^2) / 2$; where length is the longest axis or greatest longitudinal diameter and width denotes the measurement at a right angle to the length or the greatest transverse diameter (Jensen et al., 2008). Tumors of required volume, developed after about 3-4 weeks. Animals with similar tumor volumes (~80-100mm³) were grouped and subjected to treatments. In the first study, the animals were grouped as follows:

Group 1: Untreated; Group 2: Placebo treated; Group 3: Aflibercept as positive control; Group 4: VEGFR1(D1-D3)-Fc. Group 1 and 2 had three animals each, whereas, groups 3 and 4 had five animals each.

Xenografted mice in the respective groups, except for those in the control group, were injected with 200 µL formulation buffer (placebo), aflibercept, or VEGFR1(D1-D3)-Fc, subcutaneously in the opposite flank to where the implanted tumor had developed, every third day. For both VEGFR1(D1-D3)-Fc and aflibercept, a dose of 15 mg/kg body weight of mice was injected in each mice of the respective groups. Subcutaneous injections were given contralaterally twice a week for four weeks. Thus a total of eight doses were given in experimental mice. Tumor volumes were measured on each of these days when the drugs were injected. To assess *in vivo* anti-tumor activity of VEGFR1(D1-D3)-Fc and aflibercept, average tumor volumes at each time-point were plotted against duration of treatment corresponding to the days corresponding drug dosage was given.

The combinatorial effect of VEGFR1(D1-D3)-Fc with an anti-VEGF aptamer, RNV66, was tested

in the second study on A549 tumor bearing female SCID mice. In this study, the animals were grouped as follows:

Group 1: Untreated; Group 2: Placebo treated; Group 3: Aptamer; Group 4: VEGFR1(D1-D3)-Fc; Group 5: Aflibercept; Group 6: Aptamer + VEGFR1(D1-D3)-Fc. Number of animals in groups treated with aptamer and that with combination of aptamer and VEGFR1(D1-D3)-Fc was five each, whereas, the other groups except placebo, had two animals each. Three animals were grouped under placebo-control. The dosing regimen comprised three doses of aptamer (0.05 millimoles) as well as the drug combination. VEGFR1(D1-D3)-Fc dose was kept at 15 mg/kg in both drug alone and combination group. For both aflibercept and VEGFR1(D1-D3)-Fc, animals were given three doses of 15 mg/kg body weight of the animal. Experimental drug doses were given every alternate day for three doses and thereafter a treatment-free period of four weeks preceded animal sacrifice.

Three days after the last dose was injected, the animals were sacrificed by cervical dislocation and dissected to expose tumors (Overmyer et al., 2015). The sacrificed animals with tumors as well as the excised tumors were photographed. Following imaging of tumors, tumors were sectioned. Along with tumors, the other important organs (heart, brain, liver, lungs, spleen and kidneys) were also excised and collected in formalin before sectioning and subsequently subjected to Hemotoxylin and Eosin (HandE) staining.

Histopathological analysis of tumor sections

Tumors from treated xenotransplanted SCID mice were harvested and fixed with formalin and tumor tissues paraffin-embedded. Fixation was performed to preserve the tissue permanently in a near life-like state. A 10:1 ratio of fixative to tissue was used, in which, the fixative, formalin or formaldehyde (10% neutral phosphate buffered, pH 6-8) penetrates the tissue well and fixes it by cross-linking the lysine residues in particular without compromising on the protein structure or antigenicity. The formalin fixed tissue was then dehydrated using an alcohol gradient (50%, 70%, 95% and 100%), followed by treatment with a "clearing" agent (xylene) which removes the dehydrant and is miscible with the embedding agent. Tissue processor (Thermo Electron Corporation, Model-Shandon Citadel 2000) was used to perform fixation, dehydra-

tion, clearing and paraffin infiltration steps. The tissue was next embedded in paraffin using an automated tissue embedding system (Labcon, Model-Myr; California, USA). Since most tissues cannot be viewed under microscope owing to their thickness, thin sections (3–4 μm in thickness) were cut using a microtome (Thermo Electron Corporation, Model-Finesse ME, Waltham, Massachusetts, USA) and placed the sections on warm water bath to remove wrinkles from where they were picked up on glass microscopic on frosted slides. The slides with sections were left to dry overnight at room temperature for proper adhering of the tissues. Before staining, “deparaffinization” of the slides was carried out, in order to remove paraffin from the tissue and allow penetration of water-soluble dyes, by running them through xylene to alcohol gradient (100%, 95%, 70% and 50%) to water. After haematoxylin (catalogue# HHS16; Sigma-Aldrich, St. Louis, Missouri, USA) and eosin (Sigma-Aldrich; catalogue#E4382) staining using an automater stainer (Thermo Electron Corporation, Model-Veristain Gemini), the slides were washed through water to alcohol gradient (50%, 70%, 95% and 100%) to xylene and mounted with non-aqueous DPX mountant and analyzed *via* light microscopy. An Olympus BX51 microscope (Olympus, Tokyo, Japan) with ProgRes C3 image documentation camera software was used to acquire color images of HandE-stained tumor sections at 40 \times magnification.

Immunohistochemistry

Tumor and other tissues were first fixed in 15 to 20 times their volume 10% neutral buffered formalin for overnight. Fixation preserves biological tissue from decay thus averting autolysis, necrosis and putrefaction and preserves antigenicity of the tissue. However, during the process of fixation, methylene bridges are formed which cross-links proteins thereby masking the antigenic epitopes (Cooke and Losordo, 2002). Since paraffin wax is immiscible in water, the chief constituent of tissues, the tissues were dehydrated using progressively concentrated ethanol baths. This was followed by treatment with a clearing agent (xylene) which removes ethanol, after which molten paraffin infiltrates the tissue and replaces xylene. Following trimming to remove excess paraffin in order to expose the tissue, the paraffin-embedded tissues were cut in a microtome to 3–4 μm thicknesses and mounted on charged poly L-lysine coated glass slides (for HandE staining, the slides were egg albumin coated). The slides were left to dry overnight at 60°C in order to re-

move any traces of water trapped under the tissue sections, to ensure proper adherence of sections to slides and to melt the paraffin. Paraffin-embedded tissue sections were deparaffinized/ dewaxed by incubation of slides containing sections overnight at 60°C followed by immersing in xylene for 15 min. The sections were rehydrated using graded concentrations of ethanol (100%, 95%, 70% and 50%) to deionized water. The slides were kept in water and not allowed to dry from this point onwards till antigen retrieval, as dried out sections may cause non-specific antibody binding leading to high background staining. Most tissues require a step of antigen retrieval where the methylene bridges formed during fixation are broken and the antigenic sites are exposed to allow them to bind to the antibody (Cho et al., 2006). Heat-induced method of antigen retrieval was carried out using a microwave with maximum power for 5 cycles of 5 min each (with 3 cycles at 100°C and 2 cycles at 50°C) till the antigen retrieval buffer (Tris/EDTA, pH 9.0) in which the slides are placed, started to boil (Roberts, 1995). The slides were next kept under cold tap water for 10 min followed by incubation at room temperature for 30–40 min. For chromogenic method of detection, using horse radish peroxidase (HRP)-conjugated secondary antibody, a blocking step was performed to take care of endogenous peroxidase activity of cells or tissue giving rise to non-specificity. Blocking was achieved by incubating the slides with 3% H_2O_2 solution in methanol at room temperature for 20 min. For tissue sections which were used to detect Ki67 marker, using HRP-conjugated secondary antibody, blocking of endogenous peroxidase activity was performed. Following incubation with blocking agent, the slides were rinsed 4–5 times with water. A separate blocking step was used in case of CD31 detection using fluorescence with (FITC)-conjugated secondary antibody in order to avoid non-specific antibody binding and reduce background signal. Serum (100 μL) from an unrelated species (5% horse serum in Tris buffer, pH 7.4) was used as the blocking agent before addition of primary antibody and incubated for 30 min. The antibodies in horse serum (Catalogue#16050-122; Gibco) bind to the non-specific (reactive sites) of the tissue, thereby preventing non-specific binding of primary and secondary antibodies. Following incubation, the slides were rinsed with water 5 times.

Ki67 staining

The slides were incubated in Tris buffer, pH 7.4 for 5–10 min before addition of primary antibody. Tis-

sue samples were incubated with a 1:200 dilution of monoclonal mouse anti-human Ki67 antigen (Clone MIB-1; Code no. M7240; Dako, Glostrup, Denmark) (Strumfa, 2012) for 1 hr at room temperature in a humidifying chamber. The slides were rinsed 4-5 times with Tris buffer, pH 7.4. About 100 µL of peroxidase-conjugated goat anti-mouse immunoglobulin G secondary antibody (Dako REAL™ EnVision Detection System, Peroxidase/DAB+, Rabbit/Mouse; Code K5007; Dako) was added to the slides and incubated for 30 min at room temperature after which the slides were rinsed 4-5 times with Tris buffer, pH 7.4. The slides were incubated with substrate solution (DAB + Chromogen; Dako REAL kit) for 2-4 min during which a crisp brown end product is formed at the site of the target antigen. To stop the reaction, the slides were rinsed with water, following which they were counterstained with diluted hemotoxylin to analyze tissue viability and morphology, which provided a clear blue nuclear staining. The stained tissue sections were then mounted with synthetic non-aqueous mounting medium, DPX (Fischer, 2008) and viewed under a microscope (Olympus BX51) equipped with ProgRes C3 capture software.

CD31 staining

Goat anti-mouse CD31 (mouse/rat CD31/PECAM-1 affinity purified polyclonal antibody, catalogue # AF-3628, RandD Systems, Minneapolis,

Minnesota, USA) was diluted 1: 100 times in antibody diluent (catalogue# S0809, DAKO, Glostrup, Denmark) and 100 µL added to cover the entire tissue section in each slide. The slides were incubated in a humidifying chamber for 1 hr at room temperature. Following incubation, the slides were rinsed with Tris buffer, pH 7.4. Affinity purified anti-goat IgG (whole molecule)-FITC labeled polyclonal antibody produced in rabbit (catalogue# F7367, Sigma Aldrich, St. Louis, Missouri, USA) was used as secondary antibody. A 1: 400 dilution of the antibody in antibody diluent (Dako) was used followed by incubation with tissue section for 1 hr at room temperature in a humidifying chamber. The slides were rinsed with Tris buffer, pH7.4, following incubation. Sections were counterstained by incubating the slides with about 150 -200 µL of DAPI (4, 6-Diamidino-2-phenylindole dihydrochloride; catalogue# D9542, Sigma Aldrich) for 5 min in dark at room temperature followed by rinsing with buffer. The slides were washed with water and dehydrated in an increasing ethanol gradient (50%, 70%, 95% and 100%). The slides were then dried and rinsed with xylene to clear the sections. The stained tissue sections were then mounted with an aqueous mounting medium containing antifade reagent (Fluoroshield, catalogue#F6182, Sigma) to prevent rapid photobleaching of fluorescein dye. Images were viewed with a fluorescence phase contrast inverted microscope (Zeiss, Oberkochen, Germany).

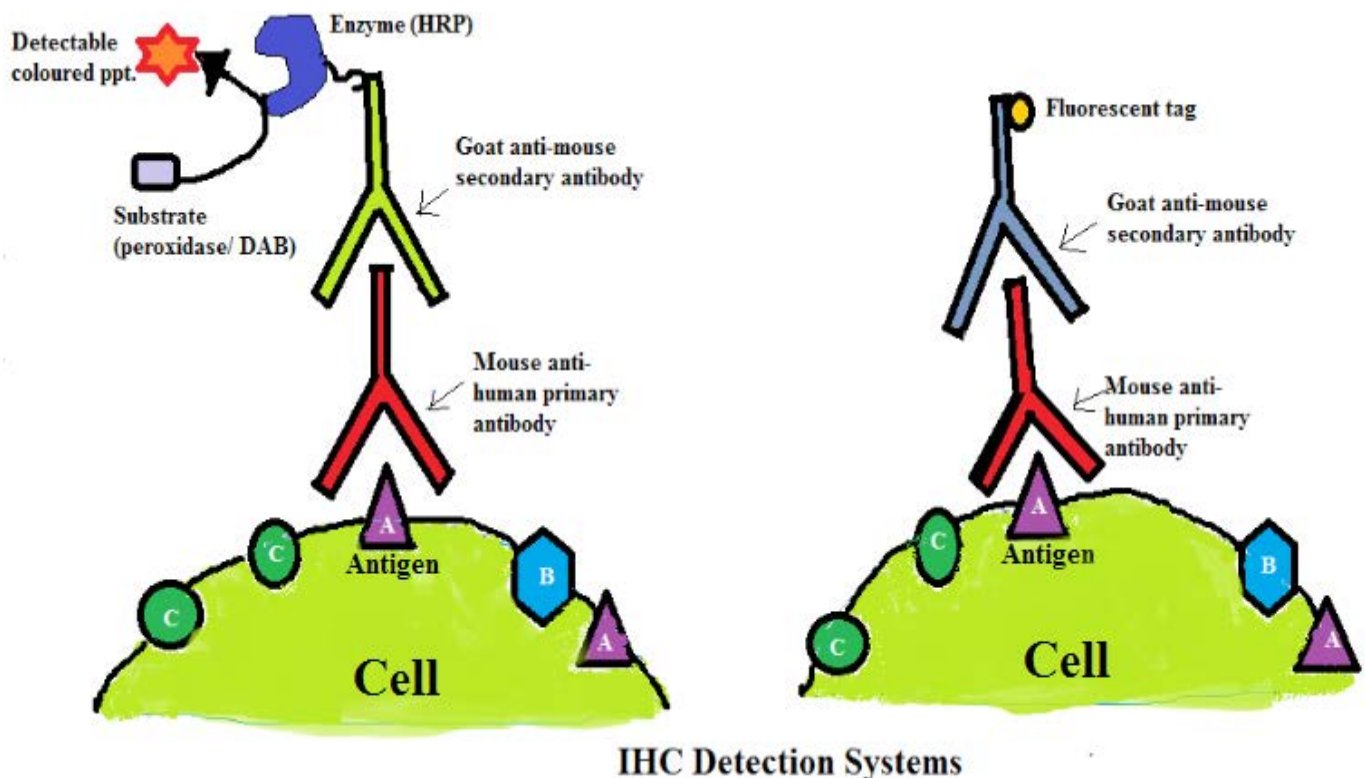


Figure 2: Immunohistochemistry scheme with different methods of antigen detection.

Statistical analyses

Raw data of tumor volume was processed to get group mean and standard deviation within each group containing 3-5 mice. Statistical differences between two groups were determined using the two-sample Student's *t*-test.

Determination of microvessel density (MVD)

Fluorescently stained sections (mouse CD31 antigen)

were microscopically examined under low (20x) and high (40x) magnification. Under low magnification, representative areas of the tumor neovascularization were marked. Under 40x magnification, ten high power fields were selected randomly within these areas and blood vessels were counted by an expert pathologist. The counts were averaged to determine the MVD of mouse CD31-positive vessels.

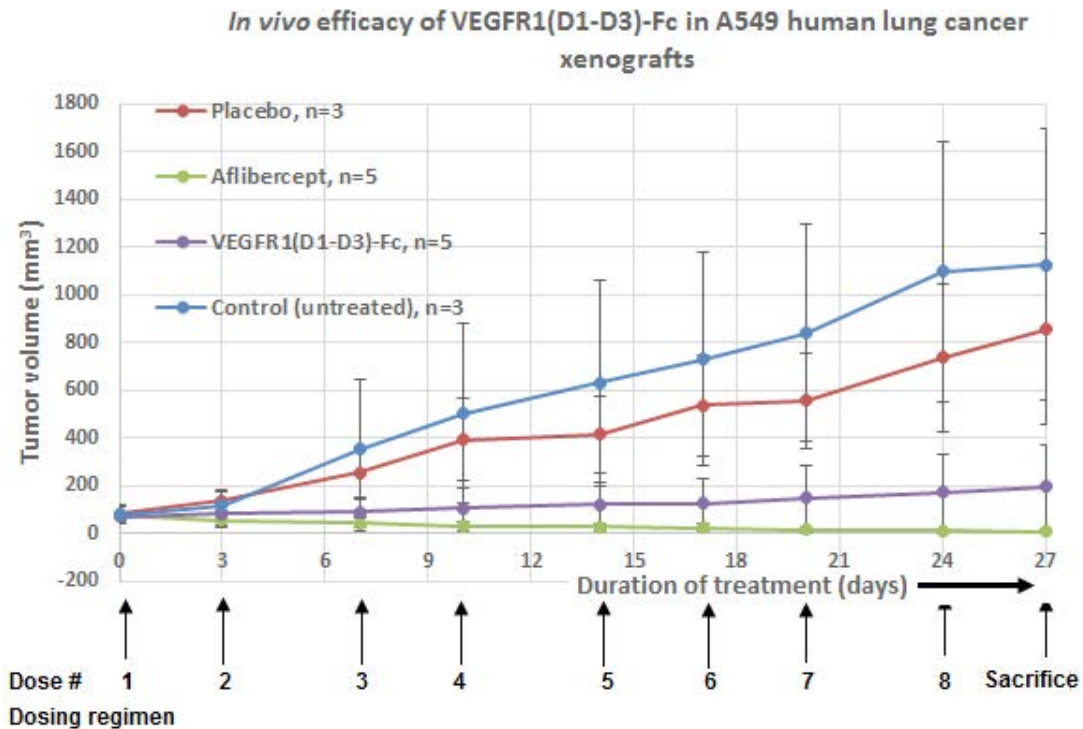


Figure 3a: Tumor growth curve in response to anti-angiogenic treatment

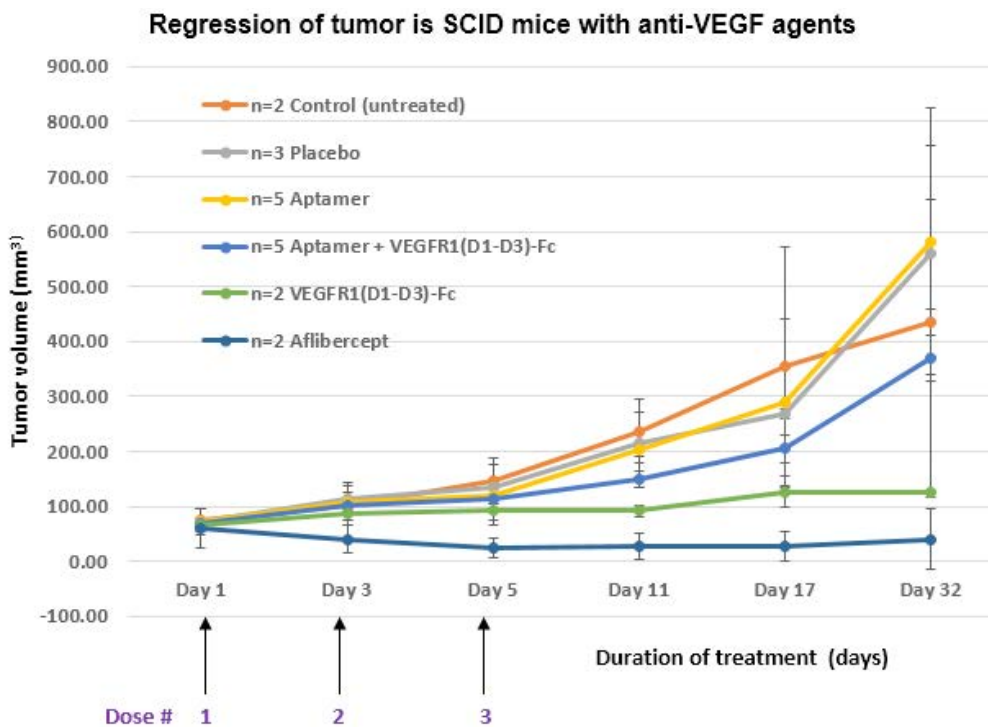


Figure 3b: Plot of mean tumor volume in SCID mice versus duration of treatment with 15 mg/kg dose of anti-VEGF molecules.

Results

Tumor volume determination

The anti-tumor effect of treatment with VEGFR1(D1-D3)-Fc was investigated in immunocompromised mice. Five million A549 human lung cancer cells were injected subcutaneously in the right flank of each of 16 six to seven weeks old male SCID mice, and tumors developed within three to four weeks to desired volume of 80–100 mm³. The mice with transplanted tumor xenografts were grouped into four clusters including untreated control, placebo-treated, positive control and test drug group. Over four weeks, a total of eight doses of 15 mg/kg body weight of animal, of anti-angiogenic proteins, VEGFR1 (D1-D3)-Fc as well as aflibercept (positive control), were subcutaneously administered to individual members of respective groups. Tumor length and width were measured every three days using digital calipers, until animals were sacrificed. Tumor volumes were calculated from length and width data using the formula: Volume = (Length × Width²)/2. It was observed that

as compared to control and placebo, there was a significant reduction in tumor volume in mice treated with aflibercept (n=5, p≤0.01). VEGFR1(D1-D3)-Fc also showed significant tumor growth inhibition after administration of the fifth dose (n=5, p≤0.01). Overall, there was an extremely slow rise in tumor volume in mice bearing xenografts over the four weeks of dosing of VEGFR1(D1-D3)-Fc, as compared to untreated or placebo-treated animals. This suggests that VEGFR1(D1-D3)-Fc has anti-tumor activity as a result of its anti-angiogenic properties as was evident from *in vitro* assays. Figures 3a and 3b show tumor growth curve and mean tumor volumes respectively, in response to anti-angiogenic treatments.

In order to investigate the anti-tumor activity of VEGFR1(D1-D3)-Fc in combination with other anti-VEGF investigational drugs, SCID mice bearing A549 tumor xenografts were treated with three doses each of VEGFR1(D1-D3)-Fc alone and anti-VEGF DNA aptamer (RNV66). It was observed that while aptamer alone was not able to reduce lung cancer tumor

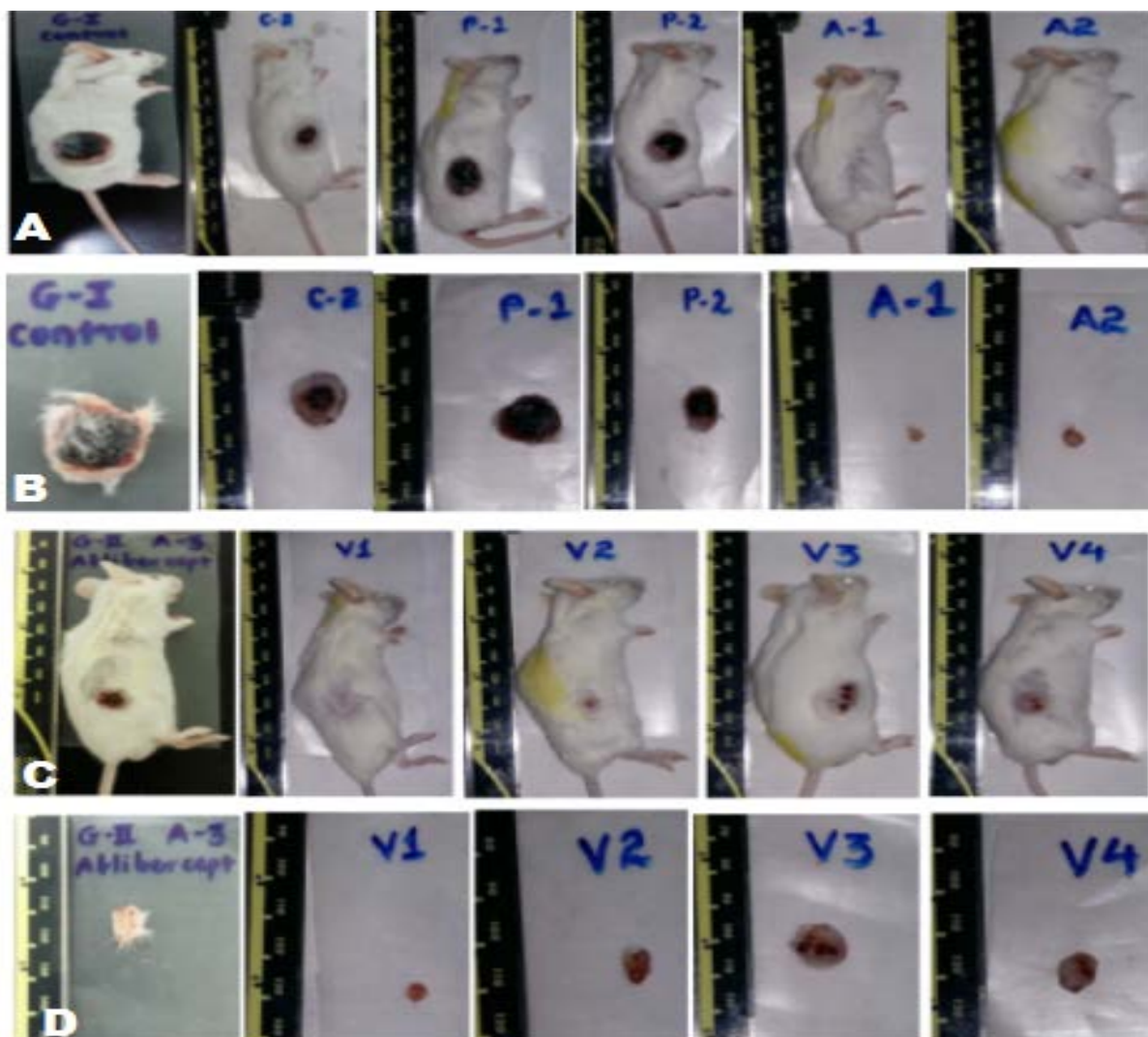


Figure 4: *In vivo* therapeutic efficacy of VEGFR1(D1-D3)-Fc to reduce xenograft tumor in SCID mice model.

burden with three administered dosages, a combination of aptamer (0.05 millimoles) and VEGFR1(D1-D3)-Fc (15 mg/kg) was able to significantly reduce tumor volume (n=5, p≤0.01) till the dosing was complete. Thereafter the combination was able to control tumor growth up till another week, after which tumor started regrowing. After completion of three doses, the anti-VEGF positive control (aflibercept), as also VEGFR1(D1-D3)-Fc, maintained the reduced tumor volume till the time of animal sacrifice, whereas it was not the case in either aptamer alone or aptamer and VEGFR1(D1-D3)-Fc combination.

The top panel A shows the mice bearing A549 human tumor xenografts, from group 1 (untreated control); where C-1 represents animal#1 and C-2 represents animal#2; group 2 (placebo-treated); where P-1 is animal#1 and P-2 is animal#2; group 3 (aflibercept-treated); where A-1 represents animal#1 and A-2 represents animal#2. The panel B represents tumors excised from the corresponding animals after sacrifice following completion of drug dosing regimen.

Mice A-3, is represented in panel C. Rest of panel C represents the mice from group 4 (VEGFR1(D1-D3)

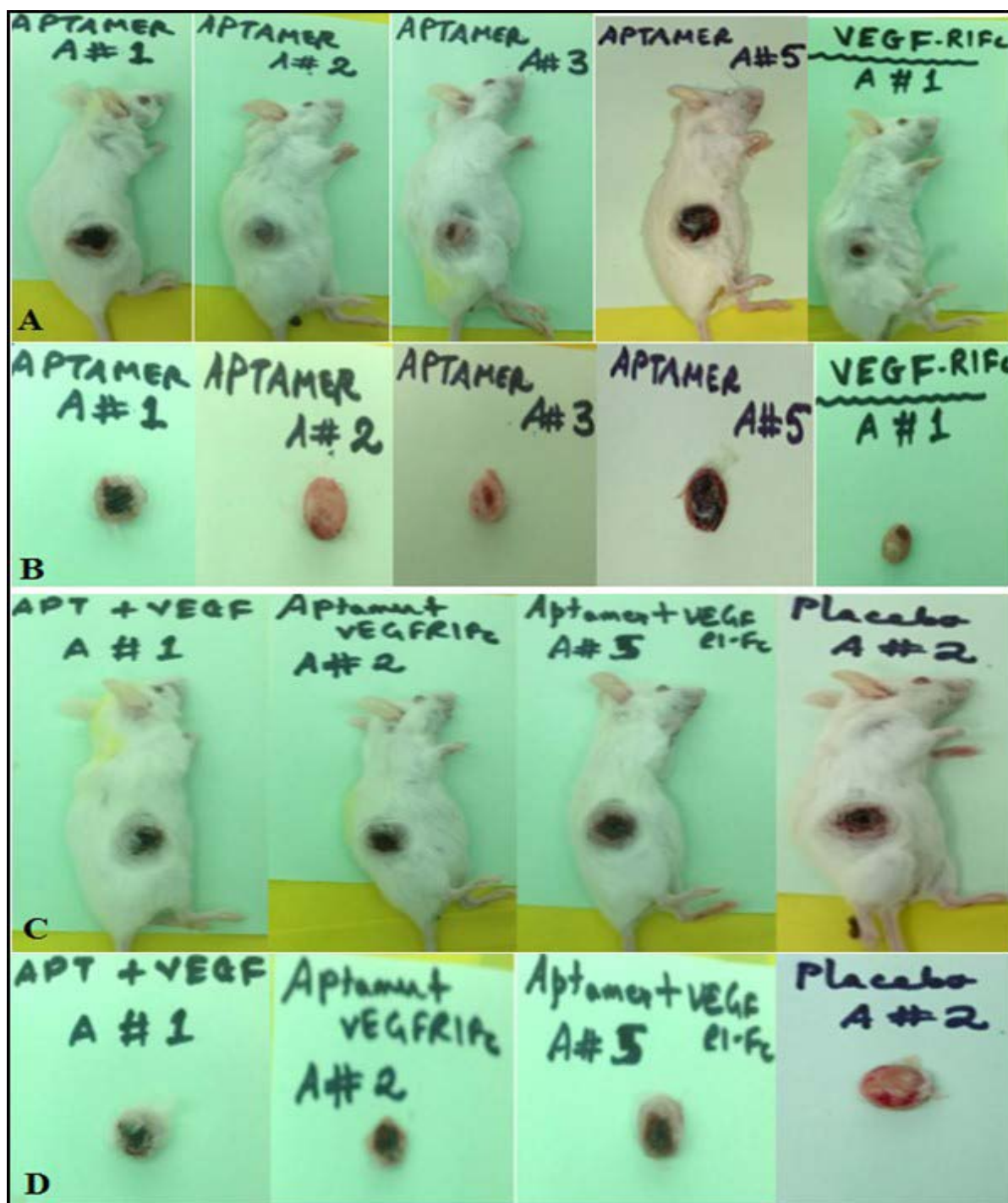


Figure 5: *In vivo* therapeutic efficacy of aptamer, RNV66 to reduce xenograft tumor in SCID mice model.

-Fc-treated); where V-1 represents animal#1, V-2 represents animal#2, V-3 represents animal#3 and V-4 represents animal#4. Panel D gives pictorial representation of excised tumors in VEGFR1(D1-D3)-Fc-treated mice. In animals V-3 and V-4, tumor size reduction is not as significant as seen in tumors excised from animals V-1 and V-2.

It can be clearly observed from Figure 4, A and B panels, that both aflibercept-treated mice (A-1 and A-2) have reduced tumor size as compared to untreated control mice and placebo. The top panel A gives pictorial representation of aptamer and VEGFR1(D1-D3)-Fc-treated SCID mice at the end of the treatment period. The panel B gives pictorial representation of excised tumors in aptamer and VEGFR1(D1-D3)-Fc-treated mice. Panel C shows pictorial representation of aptamer and VEGFR1(D1-D3)-Fc-treated SCID mice as well as placebo-treated mice at the end of the treatment period. Panel D gives pictorial representation of excised tumors in combination-treated mice as compared to placebo.

Histopathological analysis of tumors

Brightfield microscopic images of HandE stained slide from tumor section of control untreated mice, C-1, revealed the presence of 70-80% of the cells showing viable adenocarcinoma, whereas C-2 demonstrated about 60% of viable cancer cells. For the untreated control sections, mass of tumorous growth encircled by fibrous tissue was observed beneath the skin subcutaneously. Histopathological observations of surrounding skin was found within normal histological limits. Tumor mass showed predominant solid pattern of neoplastic growth. Minimal fibrous tissue proliferation along with sparse pigmentation resembling mucin, was evident in mass. Diffuse mild to moderate liquefactive necrosis was observed with nuclear dust throughout the core of tumor mass. As tumor mass showed necrosis it may be classified as invasive tumor. As tumor was induced by injecting culture of adenocarcinoma of lung, it could be classified as invasive adenocarcinoma with predominant solid mucinous pattern.

In placebo-treated mice P-1 and P-2, about 80-90% of viable tumor was detected by HandE staining of tumor. Broadly, in the placebo-treated sections, tumor mass showed minimal to moderate liquefactive necrosis. Mass was surrounded by fibrous tissue restricting further proliferation of neoplastic growth. Fibrous

tissue proliferation along with sparse pigmentation resembling mucin was evident in mass. Microscopic observation revealed minimal focal vacuolar degeneration in the mass.

Tumor sections from aflibercept-treated mice, A-2 and A-3, demonstrated small mass of tumor with only 10% and 2% of viable tumor cells respectively. Extensive necrosis and calcification was observed in A-2 while necrosis with lot of inflammatory response was observed in A-3, suggested response to the treatment. Complete tumor mass was liquefied except fibrous capsule surrounding the mass. Neoplastic growth was replaced by vacuole and adipose tissue with sparse amount of fibrovascular tissue. *Calcified foci* was observed with minimal focal mononuclear and polymorphonuclear cell infiltration.

HandE staining of VEGFR1(D1-D3)-Fc-treated tumor slide detected presence of 70-80% of viable tumor (V-3) and 60% viable tumor (V-4). Neoplastic growth was found to be restricted by surrounding with fibrous tissue. Minimal to mild multifocal liquefactive necrosis was observed. Fibrous tissue proliferation along with sparse pigmentation resembling mucin was evident in mass. Surrounding skin was found within normal histological limits. However, presence of fibrous tissue proliferation is indicative of reparative or reactive processes by tissue itself as self-limiting mechanism in response to tissue damage.

In anti-VEGF aptamer, RNV66-treated tumors, the HandE staining of sections revealed tumor mass which showed mild to moderate liquefactive necrosis with nuclear dust. Minimal mucinous pigmentation was observed with fibrous tissue proliferation. Mucinous pigmentation was more pronounced in mice, RNV66#3. This section demonstrated presence of 85% viable tumor. Focal congestion was also observed in mice, RNV66#2, which also had 85% of viable tumor. The rest 15% represented necrotic tissue.

In tumors treated with a combination of VEGFR1(D1-D3)-Fc and aptamer, RNV66, HandE staining of sections showed presence of 40-85% of viable tumor cells. Tumor mass showed moderate (about 15%) liquefactive necrosis. Fibrous tissue proliferation along with minimal mucinous pigmentation and focal calcification was evident in mass. Mucinous pigmentation was more pronounced in mice# 5, with minimal focal calcification.

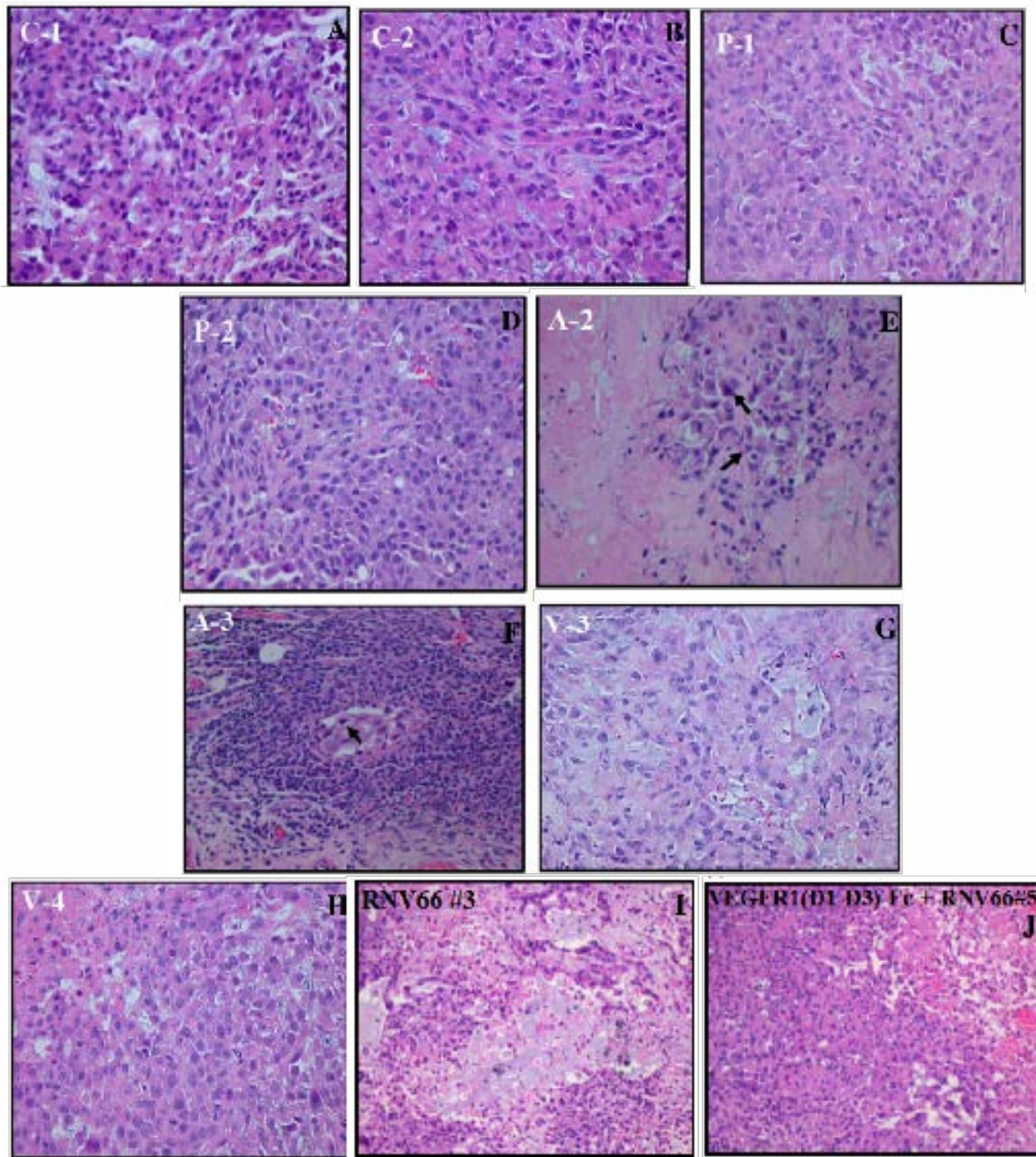


Figure 6: Representative images of histological sections of tumors.

(A, B) Images of C-1 and C-2 which represent sections from control (untreated) tumors; (C, D) Images of P-1 and P-2 which represent placebo-treated tumors; (E, F) Images of A-3 and A-4 which represent aflibercept-treated tumors; (G, H) Images of V3 and V-4 which represent VEGFR1(D1-D3)-Fc-treated tumors. (I) Image of RNV66#3, which represents aptamer-treated tumor in animal#3; (J) Image of VEGFR1(D1-D3)-Fc and RNV66# 5, which represents animal#5 which received a combination of VEGFR1(D1-D3)-Fc and aptamer, as treatment. Arrow heads indicate tumor cells in a pool of normal cells

All organs of mice (brain, heart, lungs, liver, kidney, spleen) which were evaluated by HandE staining, revealed normal histopathological findings indicating that the anti-VEGF agents did not cause acute drug-induced toxicity in the animals.

Immunohistochemical analysis

Staining of tumor sections with Ki-67 antibody

Image shows immunohistochemical staining of paraffin-embedded human A549 xenograft tumor sections

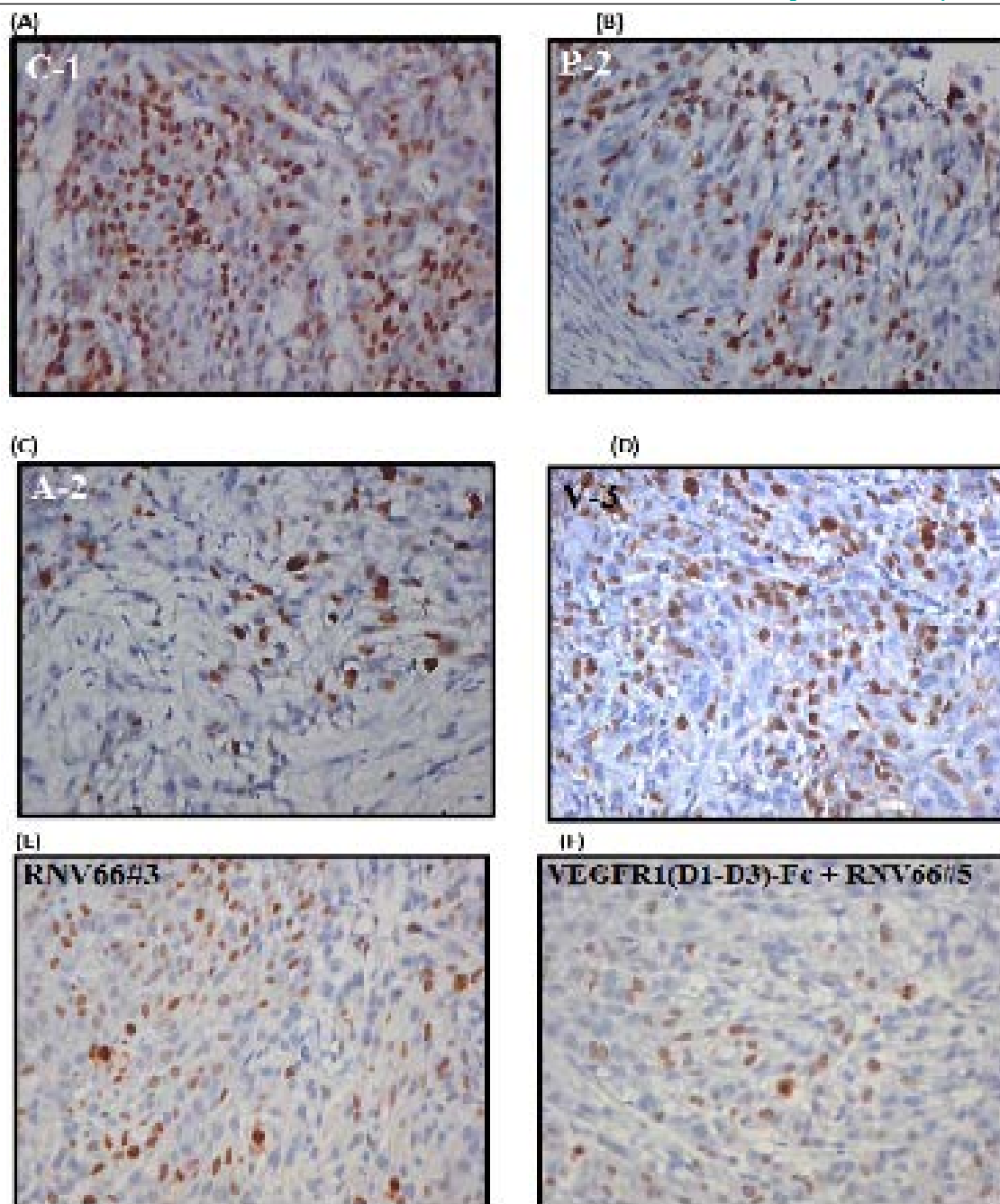


Figure 7: *Ki-67 staining of tumor sections.*

stained with anti-Ki-67 antibody using the Dako's Ki-67 clone MIB-1. Ki-67 (dark brown) displays a nuclear localization pattern which correlates its function in cell cycle progression (40X, counterstained with hematoxylin).

In control slides, C-1 as well as C-2, 60% of the tumor cells are showing Ki-67 staining in the highest proliferating region. Placebo-control slide, P-1 and P-2 however, demonstrated about 50% of tumor cells showing Ki-67 staining, as opposed to VEGFR1(D1-D3)-Fc treated tumor (slides V-3 and V-4), which showed about 40% of Ki-67 stained proliferating tumor cells. Tumors treated with aflibercept (positive

control) showed only about 10-15% of proliferating cells stained with anti-Ki-67 antibody. For tumors treated with anti-VEGF aptamer, RNV66, an average Ki-67 index of 55% was observed. A representative section from aptamer-treated animal#3 showed focally about 50% of viable tumor in the highest proliferating area. Tumor sections obtained from xenografted mice treated with a combination of VEGFR1(D1-D3)-Fc and RNV66 demonstrated a decreased 40% of viable or proliferating cells. Section obtained from animal #5, showed a Ki-67 index of 40%.

Representative slides for Ki-67 staining of tumors from each of the study groups are shown in [Figure 7](#).

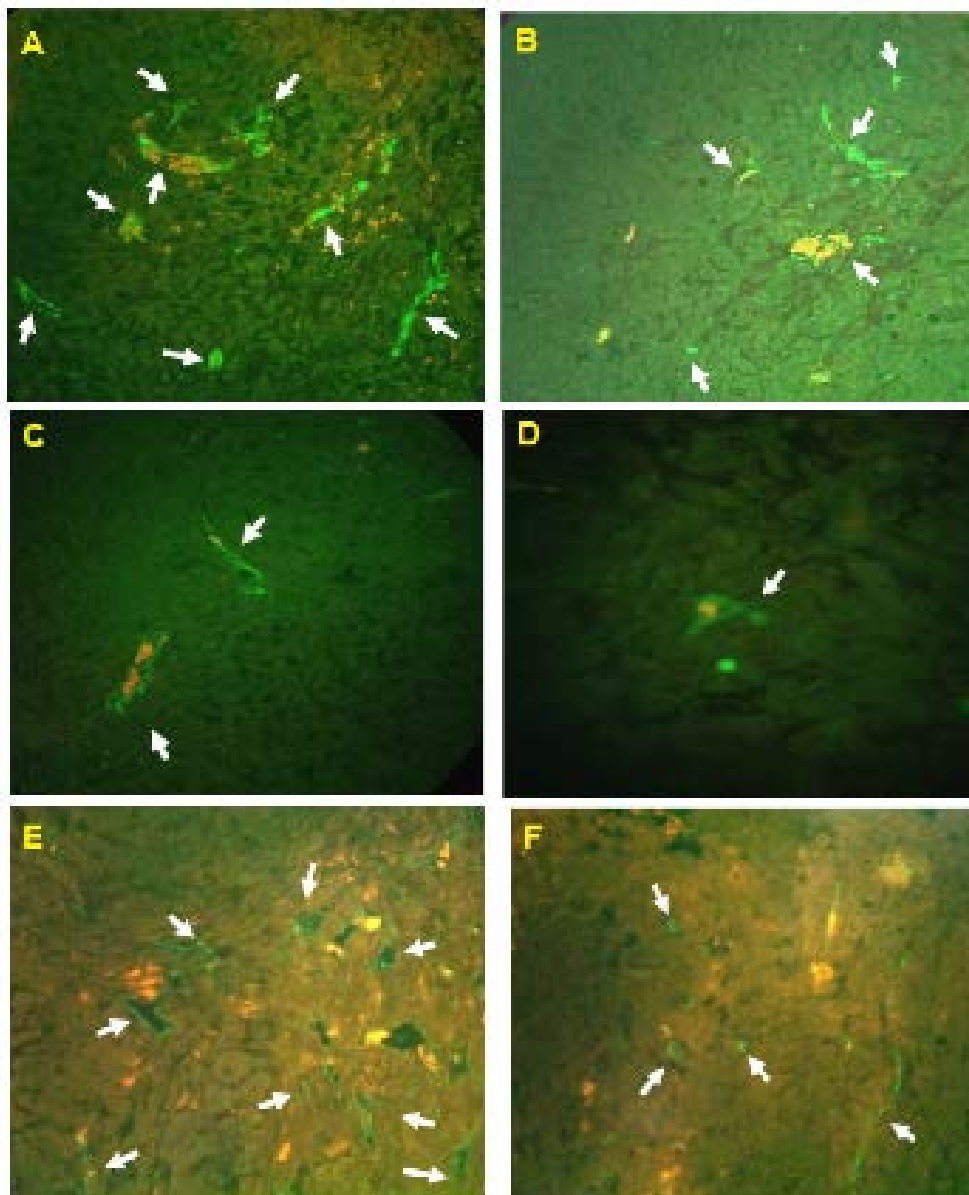


Figure 8a: Representative images of immunofluorescence staining of CD31 in mouse vasculature in tumor sections. (A) Untreated control (B) Placebo-treated (C) VEGFR1(D1-D3)-Fc-treated (D) Aflibercept-treated (E) RNV66-treated (F) VEGFR1(D1-D3)-Fc plus RNV66-treated tumor. All images were captured in high power field, under 40 x magnification. Scale bar=100 μ m.

Staining of tumor sections with mouse CD31 antibody

CD31, a vascular endothelial cell marker was detected in the newly formed or developing blood vessels supplying nutrients to the tumor, by fluorescence detection in IHC analysis. Anti-mouse CD31 antibody was used as the primary antibody in order to detect CD31 protein on mouse vascular endothelial cells, as the tumor xenograft (human in origin) is supported by blood vessels of mouse origin, with the stroma being recruited and derived from the host (Hylander et al., 2013).

From IHC images on tumor sections from untreated as well as placebo-treated controls, the CD31- immunopositive blood vessels in tumor xenograft indicate

presence of high vascularization (green FITC dye), as opposed to treated mice with VEGFR1(D1-D3)-Fc (Figure 8a (C)). This clearly demonstrates the anti-angiogenic properties of the Fc-fusion protein, whereby formation of new blood vessels is inhibited by the anti-VEGF agent, which is indicated by the reduction in the CD31 antigenic protein marker of endothelial cells. Tumors treated with aflibercept (anti-angiogenic positive control drug) showed extremely sparse population of mouse vessels, validating the anti-angiogenic effects of the drug. However, the anti-VEGF aptamer, RNV66 was unable to inhibit angiogenesis as is evident by the presence of large number of microvessels within the section of the tumor treated with the molecule. But, when a combination of VEGFR1(D1-D3)-Fc and aptamer was used to treat the

tumor, the Fc-fusion partner was able to salvage some of the anti-angiogenic property of these anti-VEGF agents and decrease blood vessel formation. As compared to Figure 8a (E), where only aptamer is used to treat the tumor, Figure 8a (F) clearly indicates a reduction in number of blood vessels in the tumor section of mice treated with the combination.

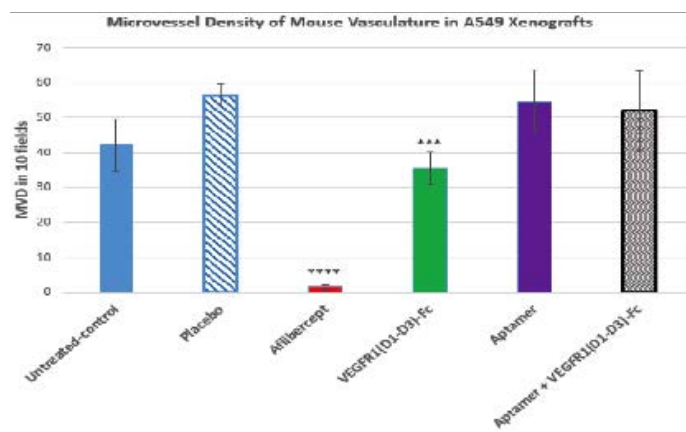


Figure 8b: Graph showing microvessel density (MVD) of tumor vasculature.

, $p \leq 0.001$; *, $p \leq 0.0001$

Microvessel density of tumor vasculature

The tumor section on each slide was viewed under microscope and individual microvessels in the entire viable section were counted manually by a trained pathologist in ten random fields under high magnification (x400). The average count was taken as a measure of microvessel density for each study group. Results were reported as the mean MVD per high-power field. Tumor sections obtained from control and placebo group of mice were observed to be well vascularized in comparison to anti-VEGF-treated tumors. Mean MVD for control (n=3) and placebo (n=3) tumors were determined to be 42.2 and 56.3 respectively. A significant reduction was observed in VEGFR1(D1-D3)-Fc-treated tumors ($p \leq 0.001$, n=5). Treatment with aflibercept, Fc-fusion protein control, revealed a remarkable reduction in microvessel formation in A549 xenografted tumors ($p \leq 0.0001$; n=5). Effect of anti-VEGF, DNA Aptamer, RNV66, was not significant in reducing tumor vasculature. Tumor sections had good vasculature in aptamer-treated samples with a mean MVD of 54, almost same as that of placebo. This result also reciprocated the tumor volume data in which the effects of treatment with aptamer as well as placebo were almost similar in terms of volume of excised tumor from SCID mice.

A combination of aptamer and VEGFR1(D1-D3)-

Fc appeared to have a synergistic effect in reducing tumor microvessels as observed from the mean MVD of 51.8, even though the effect was not overwhelming or statistically significant.

Discussion

Contribution of VEGF to tumor angiogenesis is undisputed. Several anti-VEGF agents have been already developed or under development to treat various diseases having an underlying cause of abnormal neovascularization. These anti-angiogenic molecules can be broadly classified into gene-based therapies and protein-based therapeutic agents. Gene-based therapies include use of antisense oligonucleotides, siRNA, aptamers, catalytic oligonucleotides, including ribozymes and DNAzymes and transcription decoys. Protein-based therapeutics includes monoclonal antibodies, peptidomimetics, mimetobodies, fusion proteins and decoy receptors. We have developed a Fc-fusion protein, VEGFR1(D1-D3)-Fc with minor modifications in the Fc hinge region and demonstrated its high ligand binding affinity as well as anti-angiogenic efficacy in *in vitro*²². VEGFR1(D1-D3)-Fc was shown to inhibit proliferation and capillary network formation of primary endothelial cell line (human umbilical vein endothelial cells, HUVEC) which were stimulated by VEGF₁₆₅. Similarly, DNA aptamer, RNV66, which also has very high VEGF-binding affinity, was earlier shown to efficiently inhibit proliferation of breast cancer cell line both *in vitro* and *in vivo*²⁶.

Here, we explored the *in vivo* efficacies of these anti-VEGF molecules in human lung adenocarcinoma model. Human lung cancer xenografts in immunocompromised SCID mice served as a model for studying tumor angiogenesis inhibition. In one study, 16 six to seven weeks old SCID mice were subcutaneously injected with A549 bronchoalveolar carcinoma cells. On tumor development, these animals were divided into four groups; untreated control (n=3), placebo-treated control (n=3), aflibercept-treated (n=5) and VEGFR1(D1-D3)-Fc-treated (n=5). A total of eight doses (15 mg/kg body weight) of each of the two drugs were subcutaneously administered to the mice over a period of four weeks with two injections per week. Tumor dimensions were measured at regular time points using external calipers. Significant reduction in tumor volume was observed ($p < 0.05$) in mice treated with VEGFR1(D1-D3)-Fc as compared

to mice in the placebo group, suggesting the anti-cancer activity of the protein. In the other study, SCID mice bearing A549 tumor xenografts were treated with three doses each of VEGFR1(D1-D3)-Fc (n=2), aflibercept (n=2) and RNV66 (n=5), as well as a combination of VEGFR1(D1-D3)-Fc and RNV66 (n=5). It was observed that while aptamer alone was not able to reduce lung tumor burden with the three administered doses, a combination of aptamer (0.05 millimoles) and VEGFR1(D1-D3)-Fc (15 mg/kg) was able to significantly reduce tumor volume ($p \leq 0.01$) until the last dose. Thereafter the combination was able to control tumor growth up till another week, after which tumor rebounded. In contrast, aflibercept and VEGFR1(D1-D3)-Fc, maintained the reduced tumor volume till the time of animal sacrifice. [Figure 5](#) represents *in vivo* therapeutic efficacies of different anti-angiogenic agents in SCID mice model.

Histological analysis using haematoxylin and eosin (HandE) staining was performed according to standard procedures on tumor sections. [Figure 6](#) represents images of H and E stained sections of tumor tissues. Changes in tumor growth kinetics upon treatment with aflibercept and VEGFR1(D1-D3)-Fc and aptamer RNV66, were reflected in their difference in proliferation as assessed by immunohistochemistry of cell proliferation marker, Ki-67 and angiogenesis marker, CD31. Tumor cell nucleus marker Ki-67 was stained with a primary anti-Ki-67 antibody in immunohistochemical analysis. Ki-67 reactivity, which is defined as percent tumor cells staining positive for the nuclear antigen was used as a definite marker for cell proliferation. The Ki-67 index in tumor sections of untreated and placebo-treated control mice were ~60% indicative of high tumor cell proliferation in these sections. Ki-67 index decreased for VEGFR1(D1-D3)-Fc-treated tumors to ~40% signifying inhibition of tumor cell proliferation by the Fc-fusion protein. In case of tumors treated with aflibercept (positive control), the Ki-67 cell proliferation index dropped to ~10% demonstrating the anti-proliferative and anti-cancer effects of VEGF Trap_{R1R2} molecule. In tumor treated with aptamer, RNV66, the mean Ki-67 index in highest proliferating zone of tumor section, was about 55%, indicating that the aptamer was unable to inhibit tumor cell proliferation to a large extent. However, in mice treated with a combination of VEGFR1(D1-D3)-Fc and RNV66, the proliferating tumor cells as indicated by Ki-67 staining, was slightly reduced to about 40%, which may be due to the synergistic effect

of the two anti-VEGF drugs.

Slides were stained with mouse CD31 antibody for detection of tumor blood vessel endothelial cells, as the human tumor xenograft is supported by vasculature of host mouse origin. The anti-angiogenic properties of VEGFR1(D1-D3)-Fc were demonstrated by the reduction of CD31-positive blood vessels within the tumor section obtained from SCID mice treated with VEGFR1(D1-D3)-Fc, as compared to untreated and placebo-controlled mice. Aflibercept-treated tumors demonstrated almost complete absence of mouse blood vessels in the small tumor mass, validating the known anti-angiogenic function of the molecule. [Figure 8b](#) represents a graph showing MVD of mouse vasculature in A549 xenografts. However, in A549 tumor sections of mice treated with the anti-VEGF DNA aptamer, RNV66, there was presence of plenty of CD-31 positive blood vessels indicating that the molecule was not as effective as the others as an anti-angiogenic agent. Microvessel density quantified for each of the treatments, corroborated the same findings. Since RNV66 had earlier demonstrated its anti-proliferative activity against breast cancer animal models, one possibility for its failure as an anti-tumor molecule here, may be due to the insufficient dose administered in the current study. Aptamers being much smaller in size and weight than antibodies (6-30 kD vs 150-180 kD and ~2 nm diameter vs ~15 nm diameter), are rapidly cleared by the kidneys and major organs upon entry in the bloodstream. As a result of this fast kidney filtration, aptamers have a shorter half-life *in vivo* of about 30 min for unconjugated forms, as compared to much longer circulation time in case of antibodies (upto 1 month). Hence, although aptamers have faster tissue uptake and penetration as opposed to antibodies which have limited tissue penetration, especially in solid tumors, their therapeutic efficacies may be compromised. The other major reason for failure of aptamers is degradation by serum endo and exo-nucleases. However, this vulnerability by nucleases can be reduced by modification of the phosphate backbone and sugar moieties and RNA. RNV66 has three LNA modifications which known increases its stability. Poor efficacy of RNV66 in this study is not really surprising mainly because of lower dose, its small size (7.947 KDa) and due to the fact that this molecule has been administered as naked and consequent rapid renal clearance within few minutes of administration. This can be overcome by conjugating it to bulky moiety, such as high molecu-

lar mass polyethylene glycol (PEG), cholesterol, chitosan, proteins, liposomes, organic or inorganic nanomaterials, or by multimerizing in order to create a multivalent molecule with a mass of 30-50 kD which is above the cut-off threshold for the kidney glomerulus (John et al., 2015). Conjugation at the 3' end of aptamers with biotin-streptavidin (SA) has been shown to be effective in increasing nuclease resistance and longer half life (Dougan et al., 2000). Additionally, the aptamer may be conjugated to Fc region of IgG as in VEGFR1-Fc, since any molecule with a Fc tail will most likely induce the complement lysis system and be highly effective in killing target cells. This might be via activation of the complement which is central to innate immune system system (complement dependent cytotoxicity or CDC), causing targeted cancer cell death similar to antibody mediated cellular cytotoxicity (ADCC) as a result of multiple effects such as opsonization, membrane attack complex (MAC) formation and proinflammatory anaphylatoxin release. Although, RNV66 did not show good anti-tumoricidal effects alone at the given dose, when acting in combination with VEGFR1(D1-D3)-Fc, the Fc-fusion protein was able to rescue anti-angiogenic properties of its aptamer partner to some extent, though not significantly, suggesting a strong anti-angiogenic, anti-proliferative and anti-tumor role of VEGFR1(D1-D3)-Fc.

As a forward path, the anti-angiogenic role of these promising molecules needs to be further investigated in animal models of various other human cancers. The doses of these agents and dosing regimen need to be adjusted in animal models to achieve optimal efficacy. Further, changes in the genetic level of the xenografted tumors need to be ascertained by studying the expression levels of known genes, as well as deciphering upregulated and downregulated genes in response to treatment, from global gene expression studies.

Conclusion

The functional efficacy of three different anti-VEGF molecules, one commercial Fc-fusion protein, aflibercept, one in-house developed Fc-fusion, VEGFR1(D1-D3)-Fc and an aptamer molecule, RNV66, was studied in an animal model of lung adenocarcinoma. VEGFR1(D1-D3)-Fc demonstrated significant anti-angiogenic and tumor reduction abilities in xenograft mice as compared to aflibercept. The

aptamer, which had inhibited proliferation of triple negative breast cancer cell lines in earlier studies, however, demonstrated anti-tumoral properties only in combination with the anti-angiogenic fusion protein, VEGFR1(D1-D3)-Fc. This might be due to the combination of much lower doses administered and naked injection of RNV66 without chitosan nanoparticle formulation unlike the previous report. Further *in vivo* studies would be required to establish the effectiveness of such anti-VEGF agents in different types of cancers and diseases involving angiogenesis, which may also help in designing novel combination therapies for these ailments.

Acknowledgement

The authors acknowledge the Deakin India Research Initiative (DIRI) program initiated between Reliance Institute of Life Sciences, India and Deakin University, Australia. The authors gratefully acknowledge Reliance Life Sciences Pvt. Ltd., Mumbai, India, for funding the project.

Author Contributions

Sanjukta Chakrabarti conceived, designed and performed the experiments; Sanjukta Chakrabarti, Venkata Ramana, Colin J. Barrow, Jagat R. Kanwar and Rupinder K. Kanwar analyzed the data; Sanjukta Chakrabarti wrote the paper. Rupinder K. Kanwar, Prof. Veedu and Jagat R. Kanwar proof read the manuscript and gave valuable inputs.

Conflicts of Interest

The authors declare that no conflicts of interest exists.

References

- Abhijeet, D., Kalra, P., Bansal, V., Bruno, J.G. and Sharma, K.S. 2017. Aptamer-based point-of-care diagnostic platforms. *Sensors and Actuators B: Chemical* 246, 535–553. <http://dx.doi.org/10.1016/j.snb.2017.02.060>
- Bainbridge, J.W.B., Mistry, A., M. De Alwis, Paleolog, E., Baker, A., Thrasher, A.J. and Ali, R.R. 2002. Inhibition of retinal neovascularisation by gene transfer of soluble VEGF receptor sFlt-1. *Gene therapy* 9, 320-326. <http://dx.doi.org/10.1038/sj/gt/3301680>
- Bhattacharya, R. Ye, X.C., Wang, R., Ling, X.,

- Mcmanus, M., Fan, F., Boulbes, D. and Ellis, L.M. 2016. Intracrine VEGF Signaling Mediates the Activity of Prosurvival Pathways in Human Colorectal Cancer Cells. *Cancer research* 76, 3014-3024. <http://dx.doi.org/10.1158/0008-5472.CAN-15-1605>
- Chakrabarti, S., J Barrow, C., K Kanwar, R., Ramana, V. and R Kanwar, J. 2014. Current protein-based anti-angiogenic therapeutics. *Mini reviews in medicinal chemistry* 14, 291-312. <http://dx.doi.org/10.2174/1389557514666140219114045>
 - Chakrabarti, S., Barrow, C.J., Kanwar, R.K., Ramana, V. and Kanwar, J.R. 2016. Studies to Prevent Degradation of Recombinant Fc-Fusion Protein Expressed in Mammalian Cell Line and Protein Characterization. *International Journal of Molecular Sciences* 17, 913. <http://dx.doi.org/10.3390/ijms17060913>
 - Cooke, J.P. and Losordo, D.W. 2002. Nitric oxide and angiogenesis. *Circulation* 105, 2133-2135. <https://doi.org/10.1161/01.CIR.0000014928.45119.73>
 - Cho, M-L., Jung, Y.O., Moon, Y.M., Min, S.Y., Yoon, C.H., Lee, S.H., Park, S.H., Cho, C.S., Jue, D.M. and Kim, H.Y. 2006. Interleukin-18 induces the production of vascular endothelial growth factor (VEGF) in rheumatoid arthritis synovial fibroblasts via AP-1-dependent pathways. *Immunology letters* 103, 159-166. <https://doi.org/10.1016/j.imlet.2005.10.020>
 - De Almodovar, C.R., Lambrechts, D., Mazzone, M. and Carmeliet, P. 2009. Role and therapeutic potential of VEGF in the nervous system. *Physiological Reviews*. 89, 607-648. <http://dx.doi.org/10.1152/physrev.00031.2008>
 - De Oliveira, R.L., Hamm, A. and Mazzone, M. 2011. Growing tumor vessels: more than one way to skin a cat—implications for angiogenesis targeted cancer therapies. *Mol. Asp. Med.* 32, 71-87. <http://dx.doi.org/10.1016/j.mam.2011.04.001>
 - Duffy, A.M., Bouchier-Hayes, D.J. and Harmey, J.H. 2004. Vascular endothelial growth factor (VEGF) and its role in non-endothelial cells: autocrine signalling by VEGF. *VEGF and Cancer*, 133-144. <https://www.ncbi.nlm.nih.gov/books/NBK6482/>
 - Dougan, H., Lyster, D.M., Vo, C.V., Stafford, A., Weitz, J.I. and Hobbs, J.B. 2000. Extending the lifetime of anticoagulant oligodeoxynucleotide aptamers in blood. *Nucl. Med. Biol.* 27(3), 289-97. [https://doi.org/10.1016/S0969-8051\(99\)00103-1](https://doi.org/10.1016/S0969-8051(99)00103-1)
 - Edwards, S.L., Poongavanam, V., Kanwar, J.R., Roy, K., Hillman, K.M., Prasad, N., Leth-Larsen, R., Petersen, M., Marušič, M., Plavec, J., Wengel, J. and Veedu, R.N. 2015. Targeting VEGF with LNA-stabilized G-rich oligonucleotide for efficient breast cancer inhibition. *Chemical Communications* 51, 9499-9502. <http://dx.doi.org/10.1039/c5cc02756>
 - Elshabrawy, H.A., Chen, Z., Volin, M.V., Ravela, S., Virupannavar, S. and Shahrara, S. 2015. The pathogenic role of angiogenesis in rheumatoid arthritis. *Angiogenesis* 18, 433-448. <http://dx.doi.org/10.1007/s10456-015-9477-2>
 - Ghosh, S., Basu, M. and Roy, S.S. 2012. ETS-1 protein regulates vascular endothelial growth factor-induced matrix metalloproteinase-9 and matrix metalloproteinase-13 expression in human ovarian carcinoma cell line SKOV-3. *Journal of Biological Chemistry* 287, 15001-15015. <http://dx.doi.org/10.1074/jbc.M111.284034>
 - Ghanekar, A., Ahmed, S., Chen, K. and Adeyi, O. 2013. Endothelial cells do not arise from tumor-initiating cells in human hepatocellular carcinoma. *BMC cancer* 13, 485. <http://dx.doi.org/10.1186/1471-2407-13-485>
 - Guerard, S. and Pouliot, R. 2012. The role of angiogenesis in the pathogenesis of psoriasis: mechanisms and clinical implications. *Journal of Clinical and Experimental Dermatology Research* 2012. <http://dx.doi.org/10.4172/2155-9554.S2-007>
 - Hoeben, A., Landuyt, B., Highley, M.S., Wildiers, H., Van Oosterom, A.T. and De Bruijn, E.A. 2004. Vascular endothelial growth factor and angiogenesis. *Pharmacological reviews* 56, 549-580. <https://doi.org/10.1124/pr.56.4.3>
 - Hylander, B.L., Punt, N., Tang, H., Hillman, J., Vaughan, M., Bshara, W., Pitoniak, R. and Repasky, E.A. 2013. Origin of the vasculature supporting growth of primary patient tumor xenografts. *J Transl Med* 11, 1186. <http://dx.doi.org/10.1186/1479-5876-11-110>
 - Indraccolo, S. and Mueller-Klieser, W. 2016. Potential of Induced Metabolic Bioluminescence Imaging to Uncover Metabolic Effects of Antiangiogenic Therapy in Tumors. *Frontiers in oncology* 6. <http://dx.doi.org/10.3389/fonc.2016.00015>
 - Jensen, M.M., Jørgensen, J.T., Binderup, T. and Kjær, A. 2008. Tumor volume in subcutaneous mouse xenografts measured by microCT

- is more accurate and reproducible than determined by 18F-FDG-microPET or external caliper. *BMC medical imaging* 8, 16. <http://dx.doi.org/10.1186/1471-2342-8-16>
- John G.B. 2015. Predicting the uncertain future of aptamer-based diagnostics and therapeutics. *Molecules* 20, 6866-6887. <http://dx.doi.org/10.3390/molecules20046866>
 - Kanwar, J.R., Kamalapuram, S.K. and Kanwar, R.K. 2013. Survivin signaling in clinical oncology: a multifaceted dragon. *Medicinal research reviews* 33, 765-789. <http://dx.doi.org/10.1002/med.21264>
 - Kim, J., Park, J., Choi, S., Chi, S.G., Mowbray, A.L., Jo, H. and Park, H. 2008. X-Linked Inhibitor of Apoptosis Protein Is an Important Regulator of Vascular Endothelial Growth Factor-Dependent Bovine Aortic Endothelial Cell Survival. *Circulation research* 102, 896-904. <http://dx.doi.org/10.1161/CIRCRESAHA.107.163667>
 - Krock, B.L., Skuli, N. and Simon, M.C. 2011. Hypoxia-induced angiogenesis good and evil. *Genes and cancer* 2, 1117-1133. <http://dx.doi.org/10.1177/1947601911423654>
 - Montecinos, V.P., Godoy, A., Hinklin, J., Vethanayagam, R.R. and Smith, G.J. 2012. Primary xenografts of human prostate tissue as a model to study angiogenesis induced by reactive stroma. *PLoS One* 7, e29623. <http://dx.doi.org/10.1371/journal.pone.0029623>
 - Ng, E.W., Shima, D.T., Calias, P., Cunningham, E.T. Jr., Guyer, D.R. and Adamis, A.P. 2006. Pegaptanib, a targeted anti-VEGF aptamer for ocular vascular disease. *Nature reviews drug discovery* 5, 123-132. <http://dx.doi.org/10.1038/nrd1955>
 - Ni, X., Castanares, M., Mukherjee, A. and Lupold, S.E. 2011. Nucleic acid aptamers: clinical applications and promising new horizons. *Current medicinal chemistry* 18, 4206. <http://dx.doi.org/10.2174/092986711797189600>
 - Overmyer, K.A., Thonusin, C., Qi, N.R., Burant, C.F. and Evans, C.R. 2015. Impact of anesthesia and euthanasia on metabolomics of mammalian tissues: Studies in a C57BL/6J mouse model. *PloS one* 10, e0117232. <http://dx.doi.org/10.1371/journal.pone.0117232>
 - Pidgeon, G.P., Barr, M.P., Harmey, J.H., Foley, D.A. and Bouchier-Hayes, D.J. 2001. Vascular endothelial growth factor (VEGF) upregulates BCL-2 and inhibits apoptosis in human and murine mammary adenocarcinoma cells. *British Journal of Cancer* 85, 273. <http://dx.doi.org/10.1054/bjoc.2001.1876>
 - Roy, K., Kanwar, R.K. and Kanwar, J.R. 2015. LNA aptamer based multi-modal, Fe₃O₄-saturated lactoferrin (Fe₃O₄-bLf) nanocarriers for triple positive (EpCAM, CD133, CD44) colon tumor targeting and NIR, MRI and CT imaging. *Biomaterials* 71, 84-99. <http://dx.doi.org/10.1016/j.biomaterials.2015.07.055>
 - Roberts, W.G. and Palade, G.E. 1995. Increased microvascular permeability and endothelial fenestration induced by vascular endothelial growth factor. *Journal of cell science* 108, 2369-2379.
 - Strumfa, I., Simtnece, Z., Abolins, A., Vanags, A. and Gardovskis, J. 2012. Prognostic factors after curative resection of pancreatic ductal adenocarcinoma: a retrospective study. *Journal of cancer therapeutics and research* 1, 27. <http://dx.doi.org/10.7243/2049-7962-1-27>
 - Rajappa, M., Saxena, P. and Kaur, J. 2010. Ocular angiogenesis: mechanisms and recent advances in therapy. *Advances in clinical chemistry* 50, 103-121.
 - Rubio, R.G. and Adamis, A.P. 2016. Ocular Angiogenesis: Vascular Endothelial Growth Factor and Other Factors. *Developmental Ophthalmology* 55, 28-37. <https://doi.org/10.1159/000431129>
 - Rundhaug, J.E. Matrix Metalloproteinases, Angiogenesis, and Cancer Commentary re: AC Lockhart, Braun, R.D., Yu, D., Ross, J.R., Dewhirst, M.W., Humphrey, J.S., Thompson, S., Williams, K.M., Klitzman, B., Yuan, F., Grichnik, J.M., Proia, A.D., Conway, D.A. and Hurwitz, H.I. 2003. Reduction of Wound Angiogenesis in Patients Treated with BMS-275291, a Broad Spectrum Matrix Metalloproteinase Inhibitor. *Clinical Cancer Research* 9, 551-554.
 - Smith, G.A., Fearnley, G.W., Tomlinson, D.C., Harrison, M.A. and Ponnambalam, S. 2015. The cellular response to vascular endothelial growth factors requires co-ordinated signal transduction, trafficking and proteolysis. *Bioscience reports* 35, e00253. <http://dx.doi.org/10.1042/BSR20150171>
 - Sharma, T.K., John G. B. and Abhijeet D. 2017. ABCs of DNA aptamer and related assay development. *Biotechnology advances* 35, 275-301. <http://dx.doi.org/10.1016/j.biotechadv.2017.01.003>
 - Takahashi, H. and Shibuya, M. 2005. The vascular endothelial growth factor (VEGF)/VEGF receptor system and its role under physiological

- and pathological conditions. *Clinical science* 109, 227-241. <http://dx.doi.org/10.1042/CS20040370>
- Tombran-Tink, J. and Barnstable, C.J. 2007. Ocular Angiogenesis: Diseases, mechanisms, and therapeutics. (Springer Science and Business Media, 2007). <http://www.springer.com/978-1-58829-514-9>
 - Zhou, J. and John R. 2016. Aptamers as targeted therapeutics: Current potential and challenges. *Nature Reviews Drug Discovery* 16, 181-202.